

Next-to-leading order QCD corrections to light Higgs Pair production via vector boson fusion

Terrance Figy

*Institute of Particle Physics Phenomenology, Durham University, Durham, DH1 3LE,
United Kingdom*

E-mail: terrance.figy@durham.ac.uk

ABSTRACT: We present the NLO QCD corrections for light Higgs pair production via vector boson fusion at the LHC within the CP conserving type II two higgs doublet model in the form of a fully flexible parton-level Monte Carlo program. Scale dependences on integrated cross sections and distributions are reduced with QCD K -factors of order unity.

KEYWORDS: Higgs Physics, Beyond the Standard Model, NLO Computations, QCD.

Contents

| | |
|--|----------|
| 1. Introduction | 1 |
| 2. Two Higgs Doublet Model Parameters | 2 |
| 3. The NLO Calculation | 3 |
| 4. Results for the LHC | 4 |
| 5. Conclusions | 9 |

1. Introduction

One of the primary goals of the CERN Large Hadron Collider (LHC) is a thorough investigation of the mechanism of electroweak (EW) symmetry breaking and, more specifically, the discovery of one or more Higgs bosons and the determination of their properties [1, 2]. In this context, vector-boson fusion (VBF) has emerged as particularly interesting class of processes. Higgs boson production in VBF, i.e. the EW reaction $qq \rightarrow qqh^0$, where the Higgs decay products are detected in association with two tagging jets, offers a promising discovery channel [3] and, once its existence has been verified, will help to constrain the couplings of the Higgs bosons to gauge bosons and fermions [4]. QCD corrections to the total cross section for single Higgs boson production via VBF have been computed using the structure function approach [5]. Distributions at NLO accuracy have recently become available through fully flexible parton-level Monte Carlo programs such as MCFM and VBFNLO [6, 7, 8].

The two-Higgs doublet model (THDM) predicts the existence of two neutral CP-even Higgs bosons, one neutral CP-odd Higgs boson, and two charged Higgs bosons which have selfcouplings as well as couplings to gauge bosons and fermions [9, 10]. Studies have shown that Higgs pair production at the LHC can serve as a probe of the Higgs potential [11, 12, 13]. Of interest recently has been the process $pp \rightarrow h^0 h^0 jj \rightarrow b\bar{b}b\bar{b}jj$ via VBF in the context of the two higgs doublet model [14, 15, 16, 17, 18]. It was shown in Ref. [14] that in favorable THDM scenarios that it may be possible to extract the $H^0 \rightarrow h^0 h^0 \rightarrow 4b$ resonance, thereby making the measurement of the trilinear $h^0 h^0 H^0$ coupling possible at the LHC. Assuming such a favorable scenario, the knowledge of QCD radiative corrections for this process will be needed in order to reduce the theoretical uncertainty on the total cross section and distributions. It is the aim of this paper to present the NLO QCD corrections for the process $pp \rightarrow h^0 h^0 jj \rightarrow b\bar{b}b\bar{b}jj$ via VBF in the form of a fully flexible partonic Monte Carlo program within the type II-CP conserving two higgs doublet model.

In Section 2 we give an overview of the THDM and establish benchmark points used in our simulations. Section 3 lays out the details of the NLO calculation. Cross sections and distributions for the LHC are given in Section 4. Conclusions are given in Section 5.

2. Two Higgs Doublet Model Parameters

The THDM contains two $SU(2)$ doublets, Φ_1 and Φ_2 , of weak hypercharge $Y = 1$. In the CP conserving THDM there is freedom in the choice of the Higgs boson–fermion couplings [9]: type I, in which only one Higgs doublet couples to fermions; and type II, in which the neutral member of one Higgs doublet couples to up-type quarks and the neutral member of the other Higgs doublet couples to down-type quarks and leptons. Flavor changing neutral currents (FCNC) mediated by the Higgs bosons are automatically absent in both type I and type II THDMs [19]. In this work, we only consider type II Higgs boson–fermion couplings. The most general THDM scalar potential which is invariant under $SU(2)_L \otimes U(1)_Y$ and conserves CP is given by [9],

$$\begin{aligned}
V(\Phi_1, \Phi_2) = & \lambda_1 \left(\Phi_1^\dagger \Phi_1 - v_1^2 \right)^2 + \lambda_2 \left(\Phi_2^\dagger \Phi_2 - v_2^2 \right)^2 \\
& + \lambda_3 \left[\left(\Phi_1^\dagger \Phi_1 - v_1^2 \right) + \left(\Phi_2^\dagger \Phi_2 - v_2^2 \right) \right]^2 \\
& + \lambda_4 \left[\left(\Phi_1^\dagger \Phi_1 \right) \left(\Phi_2^\dagger \Phi_2 \right) - \left(\Phi_1^\dagger \Phi_2 \right) \left(\Phi_1^\dagger \Phi_2 \right) \right] \\
& + \lambda_5 \left[\text{Re} \left(\Phi_1^\dagger \Phi_2 \right) - v_1 v_2 \right]^2 + \lambda_6 \left[\text{Im} \left(\Phi_1^\dagger \Phi_2 \right) \right]^2,
\end{aligned} \tag{2.1}$$

with two real parameters, v_1, v_2 of mass dimension one and 6 real dimensionless parameters, $\lambda_1, \dots, \lambda_6$. The minimum of the potential given by Eq. (2.1) occurs at $\Phi_i = \left(0, \frac{v_i}{\sqrt{2}} \right)^T$ for $(i = 1, 2)$. The physical spectrum of the Higgs sector of the CP-conserving THDM consists of two neutral CP even Higgs bosons, (h^0, H^0) , one neutral CP-odd Higgs boson, A^0 , and two charged Higgs bosons, (H^+, H^-) . The 8 parameters of the Higgs sector can also be taken as the vacuum expectation value, $v = \sqrt{v_1^2 + v_2^2} = \sqrt{(\sqrt{2}G_F)^{-1}}$, the masses of the Higgs bosons, $m_{h^0}, m_{H^0}, m_{A^0}$ and m_{H^\pm} , the mixing angles α and β , and λ_5 .

The parameters of the Higgs potential, Eq. (2.1), can be restricted by imposing theoretical requirements for the consistency of the model. We use, both, the requirement of vacuum stability [20] and perturbative unitarity [21] for the tree–level coupling constants. The condition of vacuum stability is given by Eq. (2) of Ref. [22]. Perturbative unitarity requires that the magnitudes of all tree–level S–wave amplitudes for elastic scattering of longitudinally polarized gauge and Higgs bosons stay in the limit set by unitarity. Here, we consider the 14 neutral channels of Ref. [23]. ρ parameter constraints from electroweak precision data have also been considered [24, 25].

In this paper, we will consider two benchmark points tabulated in Table 1 which in fact satisfy the above mentioned requirements of vacuum stability and perturbative unitarity. Benchmark point *B1* corresponds to a scenario in which the light Higgs boson does not couple to gauge bosons, i.e, $\cos(\alpha - \beta) = 1$. In this scenario it will not be possible to produce a single light Higgs via VBF since the $h^0 VV$ coupling is zero. Benchmark

point *B2* is scenario in which the heavy Higgs H^0 decouples from the gauge bosons, i.e., $\sin(\alpha - \beta) = 1$.

| | $\sin \alpha$ | $\tan \beta$ | λ_5 | m_{A^0} | m_{h^0} | m_{H^0} | m_{H^\pm} |
|-----------|---------------|--------------|-------------|-----------|-----------|-----------|-------------|
| <i>B1</i> | 0.832 | 1.50 | -3.50 | 295 GeV | 120 GeV | 300 GeV | 385 GeV |
| <i>B2</i> | -0.554 | 1.50 | 0 | 295 GeV | 120 GeV | 300 GeV | 385 GeV |

Table 1: THDM benchmark points.

3. The NLO Calculation

At leading order (LO), light Higgs pair production via VBF can, effectively, be viewed (see Fig. 1a) as the elastic scattering of two (anti)quarks, mediated by t -channel W or Z exchange, with two light Higgs boson radiated off the weak-boson propagator. The “blobs” in Fig. 1 for the process $\bar{q}Q \rightarrow \bar{q}Qh^0h^0$ represent the vector boson scattering processes $W^+W^- \rightarrow h^0h^0$ (see Fig. 2) and $ZZ \rightarrow h^0h^0$ (see Fig. 3), for charged current (CC) and neutral current (NC) processes, respectively. The generalization to crossed processes ($\bar{q} \rightarrow q$ and/or $Q \rightarrow \bar{Q}$) is straightforward. In principal we should consider the double higgstrahlung process Vh^0h^0 with $V \rightarrow q\bar{q}$ and the exchange of identical fermions in the initial or final state. However, in phase space regions with widely separated quarks jets of high invariant mass, the interference of these additional graphs is strongly suppressed by the large momentum transfer in the weak-boson propagators. Color suppression further makes these effects negligible. We, therefore, treat double higgstrahlung as a separate process and systematically neglect any identical particle effects as in the case of single Higgs boson production via VBF [26, 8]. Further, gluon fusion h^0h^0jj production is treated as a separate process, since, the $\mathcal{O}(\alpha^2\alpha_s^2)$ corrections are on the order of atobarns [27, 28].

The NLO calculation is performed in complete analogy to Ref. [6]. The real emission graphs can be obtained by attaching the gluon to the quark lines of Fig. 1a in all possible ways. Two distinct non-interfering color structures result: Feynman graphs with a single gluon attached to the upper quark line and Feynman graphs with single gluon attached to the lower quark line. Gluon initiated processes are obtained by crossing the final state gluon with the initial state (anti)quark. The result are graphs with t -channel and s -channel weak boson exchange. For consistency of the calculation we neglect the s -channel process $gq \rightarrow Vh^0h^0q$, since, we have neglected double higgstrahlung at LO.

All amplitudes are calculated numerically, using the helicity-amplitude formalism of Ref. [29]. Matrix elements for VBF proceses take the general form,

$$\mathcal{M}^{\bar{q}Q} \sim T_{VV}^{\mu\nu} J_\mu^{\bar{q}} J_\nu^Q, \quad (3.1)$$

with $J_\mu^{\bar{q}}$ and J_μ^Q being the two quark currents shown in Fig. 1. We have used the THDM implementation of FeynArts and FormCalc [30, 31] to generate model predictions for the tensors $T_{WW}^{\mu\nu}$ and $T_{ZZ}^{\mu\nu}$ for CC and NC vector boson fusion processes, respectively, for the case of off-shell vector bosons. We have introduced finite widths for h^0 and H^0 in the

s -channel Higgs propagators. The subsequent decay of the light Higgs boson h^0 to $b\bar{b}$ is performed within the narrow-width approximation.

Divergences arising from the real corrections are regulated in $d = 4 - 2\epsilon$ spacetime dimensions by using the *Catani-Seymour* dipole subtraction method [32] in the dimensional reduction scheme [33]. Formulas for the subtraction terms and finite collinear pieces are identical to the ones for single Higgs production via VBF and are given in Ref. [6].

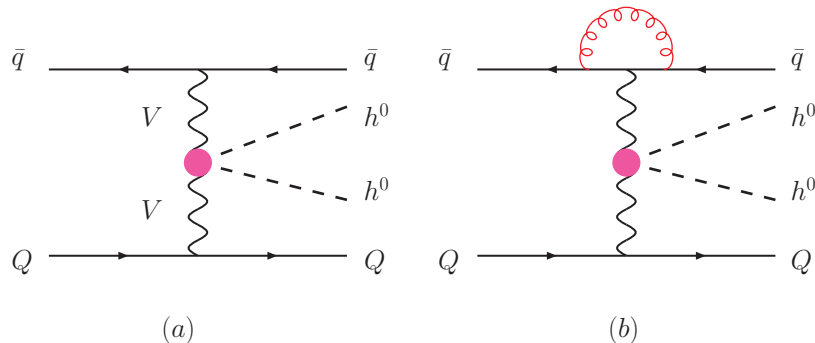


Figure 1: Feynman graphs contributing to $\bar{q}Q \rightarrow \bar{q}Qh^0h^0$ at (a) tree-level and (b) including virtual corrections to the upper line. The “blobs” correspond to VVh^0h^0 effective vertices which are represented by the tensors $T_{VV}^{\mu\nu}$ where $V = Z, W^\pm$.

4. Results for the LHC

The goal of our calculation is a precise prediction of the LHC cross section for light Higgs boson pair production in VBF with two or more jets in the context of the THDM. In order to reconstruct jets from the final-state partons, the k_T algorithm [34] as described in Ref. [35] is used, with resolution parameter $D = 0.8$. These jets are required to have

$$p_{Tj} \geq 20 \text{ GeV}, \quad |y_j| \leq 4.5. \quad (4.1)$$

Here y_j denotes the rapidity of the (massive) jet momentum which is reconstructed as the four-vector sum of massless partons of pseudorapidity $|\eta| < 5$.

At LO, there are exactly two massless final state partons. The two hardest jets are identified as tagging jets, provided they pass the k_T algorithm and the cuts described above. At NLO these jets may be composed of two partons (recombination effect) or three well-separated partons may be encountered, of which at least two satisfy the cuts of Eq. (4.1) and would give rise to either two or three-jet events. As with LHC data, a choice needs to be made for selecting the tagging jets in such a multijet situation. Here the “ p_T -method” is chosen. For a given event, the tagging jets are defined as the two jets with the highest transverse momentum with

$$p_{Tj}^{\text{tag}} \geq 30 \text{ GeV}, \quad |y_j^{\text{tag}}| \leq 4.5. \quad (4.2)$$

b -jets arising from decays of the two light Higgs bosons ($h^0 \rightarrow b\bar{b}$), are restricted by the following cuts:

$$p_{Tb} \geq 30 \text{ GeV}, \quad |\eta_b| \leq 2.5, \quad \Delta R_{jb} \geq 0.6, \quad \Delta R_{bb} \geq 0.7 \quad (4.3)$$

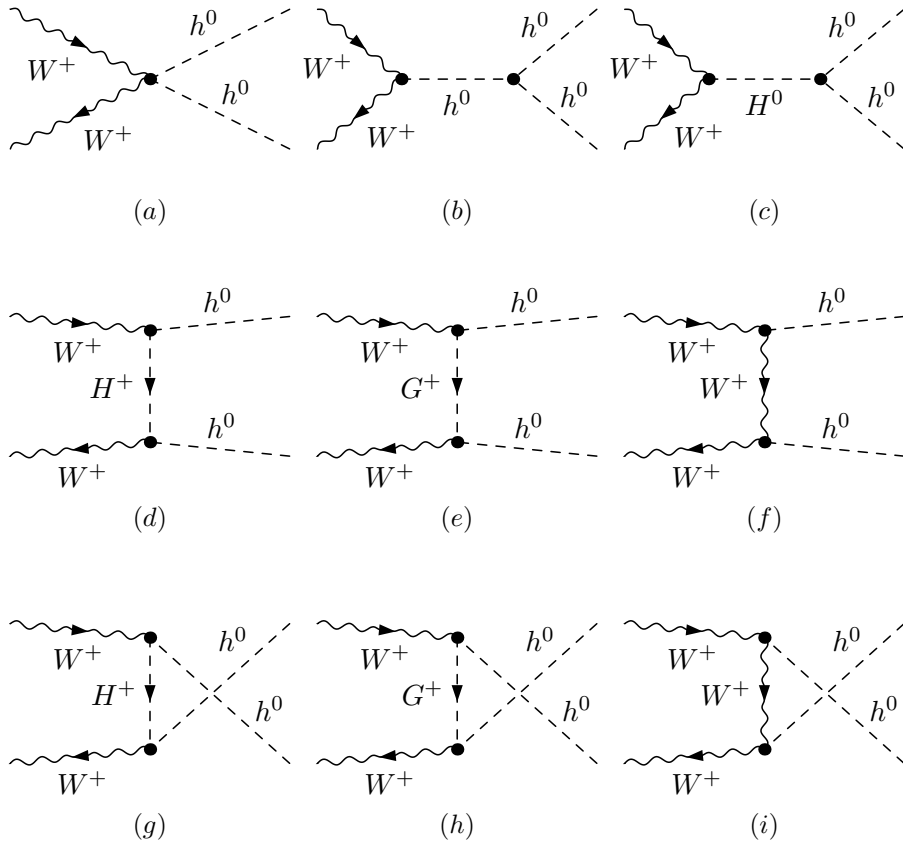


Figure 2: Feynman graphs for the process $W^+W^- \rightarrow h^0h^0$.

where ΔR_{jb} denotes the jet- b separation in the rapidity-azimuthal angle plane. In addition, the b -jets are required to fall between the two tagging jets in rapidity:

$$y_{j,\min}^{\text{tag}} < \eta_b < y_{j,\max}^{\text{tag}}. \quad (4.4)$$

Backgrounds to VBF are significantly suppressed by requiring a large rapidity separation for the two tagging jets. Tagging jets are required to reside in opposite detector hemispheres with

$$y_j^{\text{tag } 1} \cdot y_j^{\text{tag } 2} < 0 \quad (4.5)$$

and to have a large rapidity separation of

$$\Delta y_{jj} = |y_j^{\text{tag } 1} - y_j^{\text{tag } 2}| > 4, \quad (4.6)$$

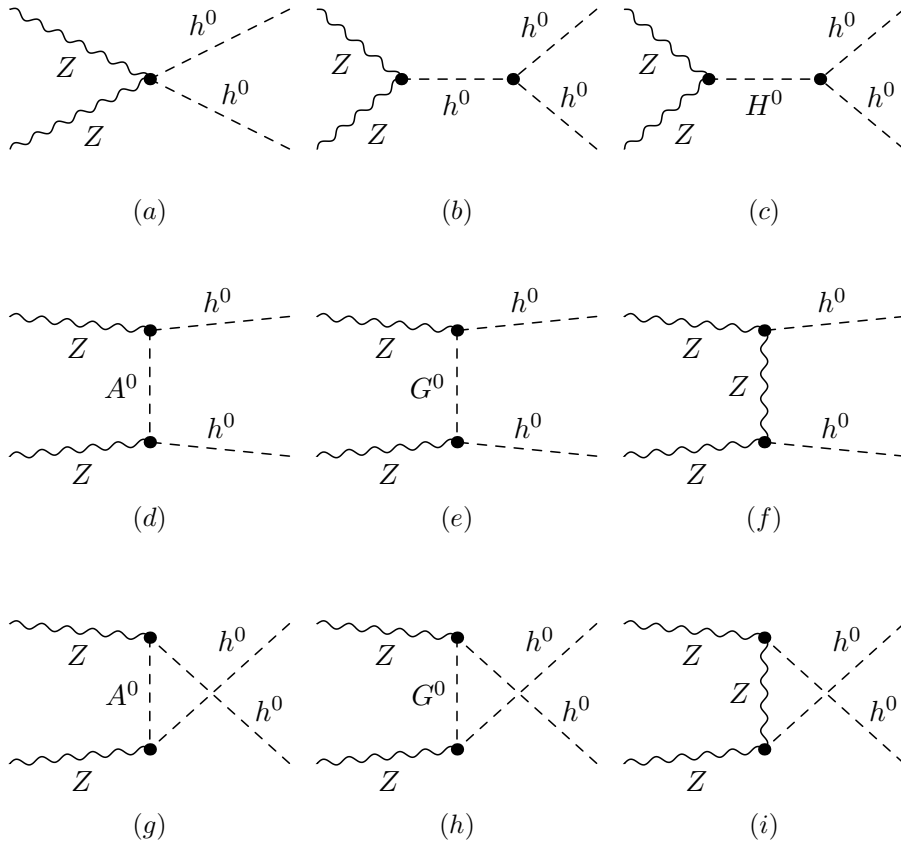


Figure 3: Feynman graphs for the process $Z^0 Z^0 \rightarrow h^0 h^0$.

sometimes called “rapidity gap cut”. QCD backgrounds can be reduced by imposing a lower bound on the invariant mass of the tagging jets of

$$m_{jj} = \sqrt{(p_j^{\text{tag } 1} + p_j^{\text{tag } 2})^2} > 600 \text{ GeV}. \quad (4.7)$$

In all subsequent calculations we use the input parameters for defining Standard Model (SM) couplings as listed in Table 2. Other SM couplings are computed using LO electroweak relations. Cross sections are computed using CTEQ6M parton distributions [36] with $\alpha_s(M_Z) = 0.118$ for all NLO results and CTEQ6L1 parton distributions with $\alpha_s(M_Z) = 0.130$ for all leading order cross sections. The running of the strong coupling is evaluated at two-loop order for all NLO results. In the following we use benchmark point *B1* for NLO and LO Monte Carlo simulations.

In Figures 4 and 5, we show the scale dependence of the total cross section within the cuts of Eqs. (4.1)-(4.7) for the process $pp \rightarrow h^0 h^0 jj \rightarrow b\bar{b}b\bar{b}jj$ via VBF at the LHC.

Scale variations are shown for (a) LO results with $\mu_F = \xi\mu_0$ (black dotted line), (b) NLO results with $\mu_F = \xi\mu_0$ and $\mu_R = \mu_0$ (blue dot-dashed line), (c) NLO results with $\mu_R = \xi\mu_0$ and $\mu_F = \mu_0$ (green dashed line), and (d) LO results with $\mu_F = \xi\mu_0$ (red solid line). In Figure 4, we choose a fixed reference scale, $\mu_0 = 2m_h$. In Figure 5, we choose the reference scale to be the virtuality of the exchanged t -channel vector boson, q_V , shown in Figure 1. For $\mu_F = \xi\mu_0$ with $0.2 < \xi < 5$ the scale variation of the LO cross section is +19% to -14% for both choices of reference scale μ_0 . While at NLO, the scale variations are -1.34% to -2.64% for $\mu_F = \mu_R = 5^{\pm 1}(2m_h)$ and -5% to 0.5% for $\mu_F = \mu_R = 5^{\pm 1}q_V$. Table 3 lists total cross sections at NLO for the benchmark scenarios of Table 1. For benchmark $B2$ the cross section is below 1 femtobarn due to the fact that the heavy Higgs boson does not couple to gauge bosons.

Our Monte Carlo program allows the analysis of arbitrary infrared and collinear safe distributions with NLO QCD accuracy. In order to assess the impact of the NLO corrections we compare LO and NLO results by plotting the dynamical K factor

$$K(x) = \frac{d\sigma_3^{NLO}(\mu_R = \mu_F = \mu_0)/dx}{d\sigma_3^{LO}(\mu_R = \mu_F = \mu_0)/dx} \quad (4.8)$$

for our reference scale of μ_0 . The stability of the results is represented via the scale dependence, given by the ratio of cross sections,

$$R(x) = \frac{d\sigma_3(\mu_R = \mu_F = \xi\mu_0)/dx}{d\sigma_3(\mu_R = \mu_F = \mu_0)/dx}. \quad (4.9)$$

We plot results for $\xi = 1/2$ and 2 with $\mu_0 = q_V$ for NLO and LO distributions.

Figure 6 shows the maximum transverse momentum of the two tagging jets defined as $p_{T,tag}^{\max} = \max(p_T^{\text{tag } 1}, p_T^{\text{tag } 2})$. The left panel shows the distribution at LO (dashed green histogram) and at NLO (solid red histogram). The right panel shows phase space dependent K factor (solid green histogram).

Scale variations $\mu_R = \mu_F = \xi\mu_0$ for $\xi = 0.5$ and 2 are shown for LO (dotted histograms) and NLO (dashed histograms). While at LO the scale variations are $\pm 8\%$, they are reduced to $\pm 1\%$ at NLO. Figure 9 shows the rapidity separation of the two tagging jets. At NLO the tagging jet rapidity separation tends to increase which is typical behavior for VBF production processes [6].

| Benchmark | $\sigma_{LO}(\text{fb})$ | $\sigma_{NLO}(\text{fb})$ | K -factor |
|-----------|--------------------------|---------------------------|-------------|
| $B1$ | 86.87 | 87.62 | 1.0086 |
| $B2$ | 0.1864 | 0.1858 | 0.9969 |

Table 3: Integrated LO cross sections, σ_{LO} , NLO cross sections, σ_{NLO} , in femtobarns (fb). The QCD K -factors are defined as $K = \sigma_{NLO}/\sigma_{LO}$. The renormalization and factorization scale has been set to $\mu_R = \mu_F = q_V$.

| M_Z | M_W | G_F |
|------------|------------|---------------------------------------|
| 91.188 GeV | 80.416 GeV | $1.16639 \times 10^{-5}/\text{GeV}^2$ |

Table 2: SM input parameters

Figure 7 shows the distribution in the maximum transverse momentum of the four b -jets resulting from the decay of the light Higgs bosons defined as $p_{T,b}^{\max} = \max(p_{T,b1}, \dots, p_{T,b4})$. The distribution is peaked in the vicinity of 100 GeV because we have chosen the light Higgs boson mass to be $m_h = 120$ GeV. A lower light Higgs mass would result in a softer b -jet. Figure 8 shows the distribution in the four b -jet invariant mass, $m_{4b} = \sqrt{(p_{b1} + \dots + p_{b4})^2}$. A peak occurs around the mass of the heavy Higgs boson, $m_H = 300$ GeV. In both distributions the scale dependence is reduced with relatively flat phase space dependent K factors.

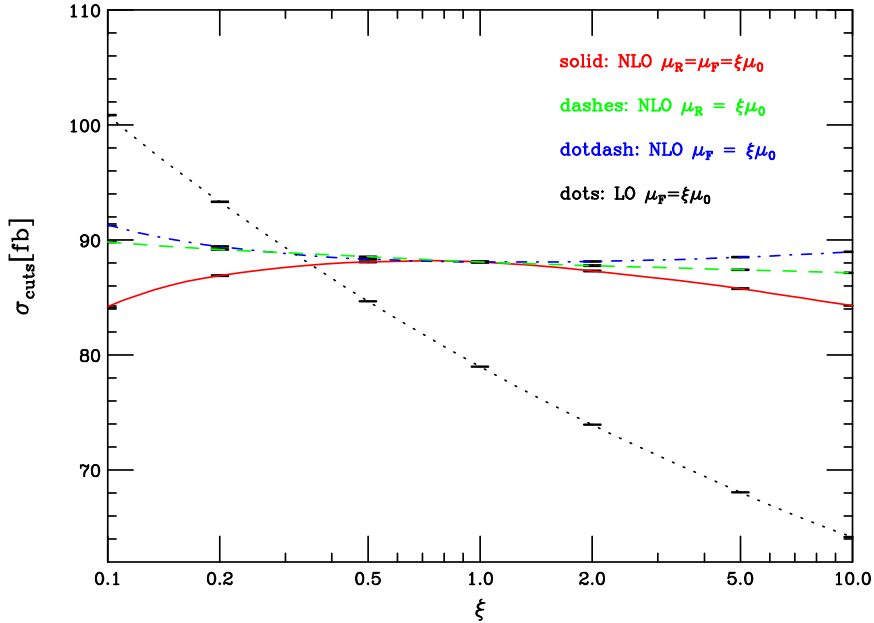


Figure 4: Scale dependence of the total cross section at LO and NLO within the cuts of Eqs. (4.1)-(4.7) for VBF $h^0 h^0 jj$ production at the LHC. The factorization scale μ_F and the renormalization scale μ_R are taken as multiples, $\xi\mu_0$, of the fixed reference scale $\mu_0 = 2m_h$. The NLO curves are for $\mu_R = \mu_F = \xi\mu_0$ (solid red line), $\mu_F = \mu_0$ and $\mu_R = \xi\mu_0$ (dashed green line), and $\mu_F = \xi\mu_0$ and $\mu_R = \xi\mu_0$ (dot-dashed blue line). The dotted black curve shows the scale dependence of the LO cross section for $\mu_F = \xi\mu_0$.

In Figure 10, we show the normalized azimuthal angle correlation of the tagging jets, $\Delta\phi_{jj}$, for benchmark points $B1$ and $B2$. Here $\Delta\phi_{jj} = \phi_{j+} - \phi_{j-}$ with j_+ (j_-) being the “toward” (“away”) jet as defined in Ref. [37]. For benchmark $B1$, the normalized distribution in $\Delta\phi_{jj}$ has the characteristic shape for single H^0 production followed by the decay, $H^0 \rightarrow h^0 h^0$ where the tensor structure of the HVV vertex is $g^{\mu\nu}$ [37, 38]. However, for benchmark $B2$ in which the H^0 is decoupled from the gauge bosons the shape of the $\Delta\phi_{jj}$ distribution develops a peak at $\Delta\phi_{jj} = 0$ degrees as opposed to a dip.¹ This is due to the interference of s -channel and t -channel $VV \rightarrow h^0 h^0$ graphs.

¹Such features have been pointed out in Ref. [39] for slepton pair production via VBF.

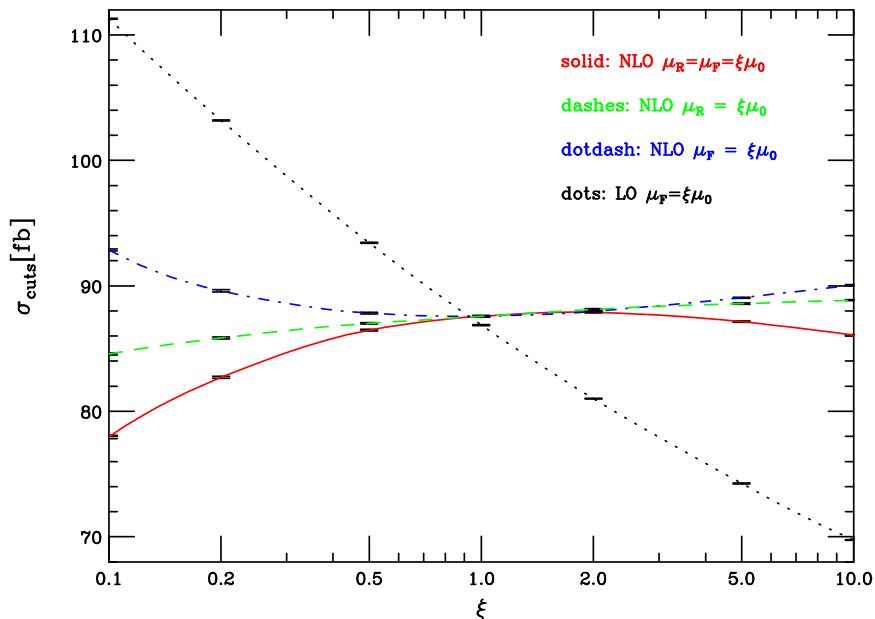


Figure 5: The caption is the same as in Fig. 4 except $\mu_0 = q_V$.

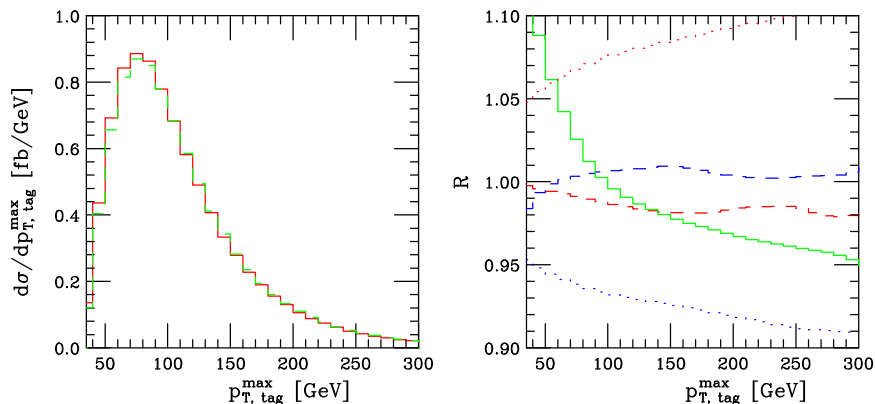


Figure 6: Maximum transverse momentum of the two tagging jets. In the left panel, $d\sigma/dp_{T, \text{tag}}^{\text{max}}$ is shown at LO (dashed green) and NLO (solid red) for $\mu_0 = q_V$. The right-hand panel depicts the K factor (solid green) and scale variations of LO (dotted) and NLO (dashed) results for $\mu_R = \mu_F = \xi\mu_0$ with $\xi = 1/2$ and 2.

5. Conclusions

We have computed the next-to-leading order QCD corrections for light Higgs pair production via vector boson fusion at the LHC within the type II CP conserving two-higgs doublet model. We have included the subsequent decay of the light Higgs to the $b\bar{b}$ final state. Our NLO calculation takes the form of a fully flexible partonic Monte Carlo program allowing arbitrary phase space cuts. We have shown that scale variations for total cross sections and distributions are reduced at NLO. QCD K -factors are modest. These results are consistent with those of Standard Model Higgs production via vector boson fusion [6].

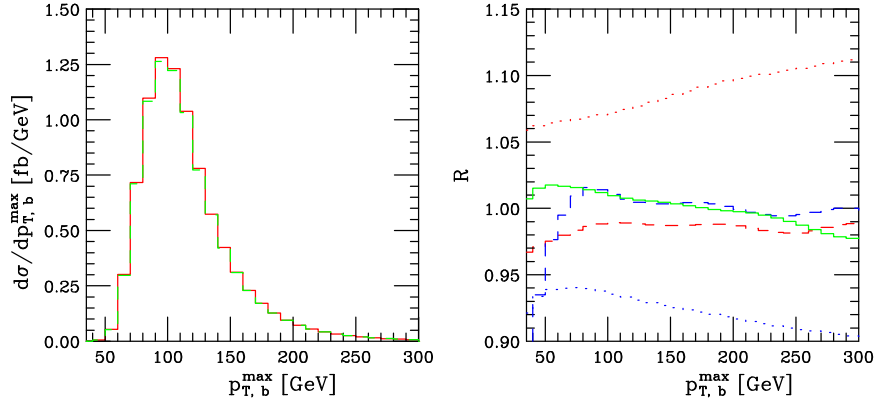


Figure 7: Maximum transverse momentum of the four b jets. In the left panel, $d\sigma/dp_{T,b}^{\max}$ is shown at LO (dashed green) and NLO (solid red) for $\mu_0 = q_V$. The right-hand panel depicts the K factor (solid green) and scale variations of LO (dotted) and NLO (dashed) results for $\mu_R = \mu_F = \xi\mu_0$ with $\xi = 1/2$ and 2.

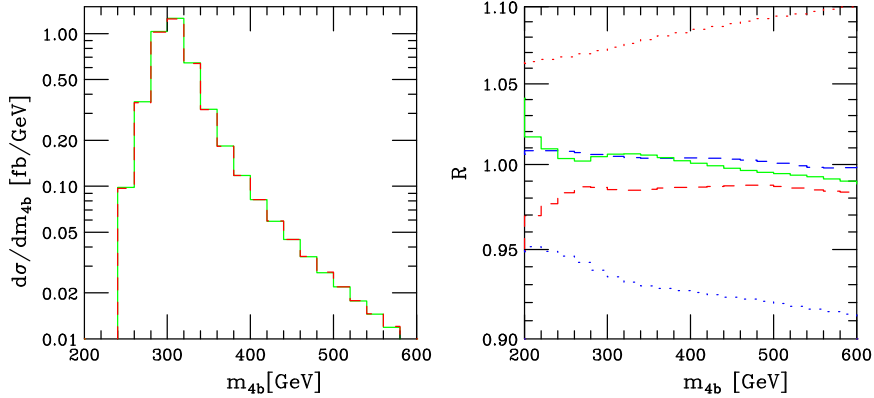


Figure 8: The four b -jet invariant mass, $m_{4b}^2 = (p_{b,1} + p_{b,2} + p_{b,3} + p_{b,4})^2$. In the left panel, $d\sigma/dm_{4b}$ is shown at LO (dashed green) and NLO (solid red) for $\mu_0 = q_V$. The right-hand panel depicts the K factor (solid green) and scale variations of LO (dotted) and NLO (dashed) results for $\mu_R = \mu_F = \xi\mu_0$ with $\xi = 1/2$ and 2.

We also note the sensitivity of the azimuthal angle correlation of the two tagging jets, $d\sigma/d\Delta\phi_{jj}$, to the tensorial structure of $VV \rightarrow h^0 h^0$ scattering amplitudes. For THDM scenarios in which the heavy Higgs coupling to electroweak gauge bosons is highly suppressed, the $\Delta\phi_{jj}$ distribution is peaked at $\Delta\phi_{jj} = 0$ degrees while for scenarios in heavy Higgs couples to electroweak gauge bosons there is a dip at $\Delta\phi_{jj} = 0$ degrees.

Acknowledgments

Work supported in part by the European Community's Marie-Curie Research Training Network under contract MRTN-CT-2006-035505 'Tools and Precision Calculations for Physics Discoveries at Colliders'. TF would like to thank Oliver Brein and Dieter Zeppenfeld for discussions concerning this project. All numerical computations presented in this paper were performed via PhenoGrid using GridPP infrastructure.

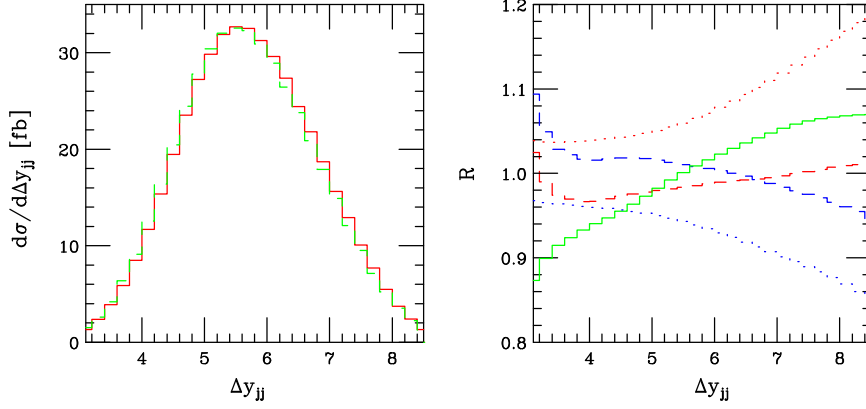


Figure 9: Rapidity separation within the cuts of Eqs. (4.1)-(4.7). In the left panel, $d\sigma/dy_{jj}$ is shown at LO (dashed green) and NLO (solid red) for $\mu_0 = q_V$. The right-hand panel depicts the K factor (solid green) and scale variations of LO (dotted) and NLO (dashed) results for $\mu_R = \mu_F = \xi\mu_0$ with $\xi = 1/2$ and 2.

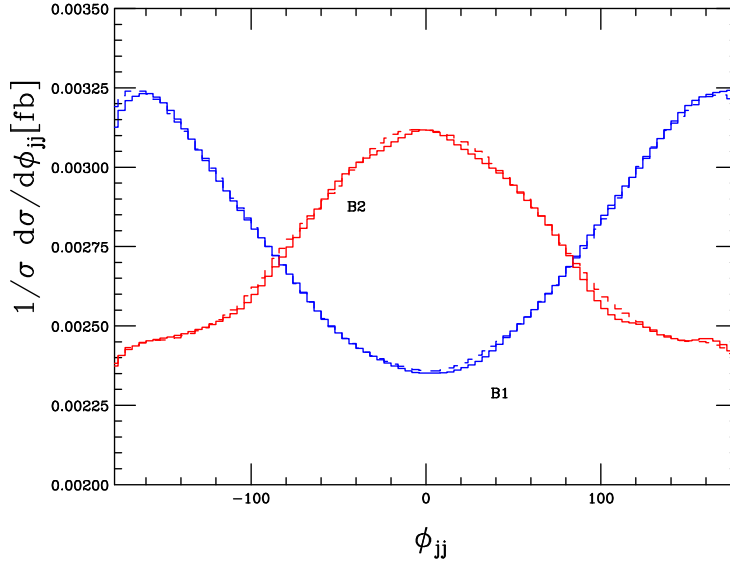


Figure 10: The normalized distribution in azimuthal angle correlation of the two tagging jets, $\frac{1}{\sigma} \frac{d\sigma}{d\Delta\phi_{jj}}$, for benchmark scenarios $B1$ (red) and $B2$ (blue) at NLO (solid) and LO (dashed).

References

- [1] ATLAS Collaboration, ATLAS TDR, ATLAS Detector and Physics Performance Technical Design Report, Report No. CERN/LHCC/99-15 (1999); E. Richter-Was and M. Sapinski, “Search for the SM and MSSM Higgs boson in $t\bar{t}H, H \rightarrow b\bar{b}$ channel,” *Acta Phys. Polon.* **B30** (1999) 1001; B. P. Kersevan and E. Richter-Was, “What is the $Wb\bar{b}, Zb\bar{b}$ or $t\bar{t}b\bar{b}$ irreducible background to the light-Higgs boson searches at LHC?” *Eur. Phys. J.* **C 25** (2002) 379 [[hep-ph/0203148](#)].
- [2] G. L. Bayatian *et al.*, CMS Technical Proposal, Report No. CERN/LHCC/94-38x (1994); D. Denegri, “Prospects for Higgs (SM and MSSM) searches at LHC,” talk in the Circle Line Tour Series, Fermilab, October 1999, (<http://www-theory.fnal.gov/CircleLine/DanielBG.html>); R. Kinnunen and D. Denegri, “Expected SM/SUSY Higgs observability in CMS,” CMS Note No. 1997/057; R. Kinnunen and A. Nikitenko, “Study of $H_{SUSY} \rightarrow \tau\tau \rightarrow l^\pm + h^\mp + E_t^{miss}$ in CMS,” Report No. CMS TN/97-106; R. Kinnunen and D. Denegri, “The $H_{SUSY} \rightarrow \tau\tau \rightarrow h^\pm + h^\mp + X$ channel, its advantages and potential instrumental drawbacks,” [hep-ph/9907291](#); V. Drollinger, T. Müller and D. Denegri, “Searching for Higgs Bosons in Association with Top Quark Pairs in the $H \rightarrow b\bar{b}$ Decay Mode,” [hep-ph/0111312](#).
- [3] D. L. Rainwater, PhD thesis, “Intermediate-mass Higgs searches in weak-boson fusion,” [hep-ph/9908378](#).
- [4] D. Zeppenfeld, R. Kinnunen, A. Nikitenko and E. Richter-Was, “Measuring Higgs boson couplings at the LHC,” *Phys. Rev.* **D 62** (2000) 013009 [[hep-ph/0002036](#)]; D. Zeppenfeld, “Higgs couplings at the LHC,” in *Proc. of the APS/DPF/DPB Summer Study on the Future of Particle Physics, Snowmass, 2001* edited by N. Graf, eConf **C010630**, (2001) 123 [[hep-ph/0203123](#)]; A. Belyaev and L. Reina, “ $pp \rightarrow t\bar{t}H, H \rightarrow \tau^+\tau^-$: Toward a model independent determination of the Higgs boson couplings at the LHC,” *J. High Energy Phys.* **08** (2002) 041 [[hep-ph/0205270](#)]; M. Dührssen *et al.*, S. Heinemeyer, H. Logan, D. Rainwater, G. Weiglein and D. Zeppenfeld, “Extracting Higgs boson couplings from LHC data,” *Phys. Rev.* **D 70** (2004) 113009 [[hep-ph/0406323](#)].
- [5] T. Han, G. Valencia and S. Willenbrock, “Structure function approach to vector boson scattering in p p collisions,” *Phys. Rev. Lett.* **69** (1992) 3274 [[hep-ph/9206246](#)].
- [6] T. Figy, C. Oleari and D. Zeppenfeld, “Next-to-leading order jet distributions for Higgs boson production via weak-boson fusion,” *Phys. Rev. D* **68** (2003) 073005 [[arXiv:hep-ph/0306109](#)].
- [7] E. L. Berger and J. Campbell, “Higgs boson production in weak boson fusion at next-to-leading order,” *Phys. Rev. D* **70** (2004) 073011 [[hep-ph/0403194](#)].
- [8] M. Ciccolini, A. Denner and S. Dittmaier, “Strong and electroweak corrections to the production of Higgs+2jets via weak interactions at the LHC,” *Phys. Rev. Lett.* **99** (2007) 161803 [[arXiv:0707.0381](#)]; “Electroweak and QCD corrections to Higgs production via vector-boson fusion at the LHC,” *Phys. Rev. D* **77** (2008) 013002 [[arXiv:0710.4749](#) [[hep-ph](#)]].
- [9] J. F. Gunion, H. E. Haber, G. L. Kane and S. Dawson, “THE HIGGS HUNTER’S GUIDE,” Addison-Wesley Publishing Company, 1990 [Erratum [hep-ph/9302272](#)]; H. Georgi, *Hadronic. J.* **1** (1978) 155.
- [10] J. F. Gunion and H. E. Haber, “The CP-conserving two-Higgs-doublet model: The approach to the decoupling limit,” *Phys. Rev. D* **67** (2003) 075019 [[arXiv:hep-ph/0207010](#)].

- [11] M. Moretti, S. Moretti, F. Piccinini, R. Pittau and A. D. Polosa, “Beyond the standard model Higgs boson self-couplings at the LHC,” arXiv:hep-ph/0411039.
- [12] M. Moretti, S. Moretti, F. Piccinini, R. Pittau and A. D. Polosa, “Higgs boson self-couplings at the LHC as a probe of extended Higgs sectors,” *JHEP* **0502** (2005) 024 [arXiv:hep-ph/0410334].
- [13] F. Boudjema and A. Semenov, “Measurements of the SUSY Higgs self-couplings and the reconstruction of the Higgs potential,” *Phys. Rev. D* **66** (2002) 095007 [arXiv:hep-ph/0201219].
- [14] M. Moretti, S. Moretti, F. Piccinini, R. Pittau and J. Rathsman, “Vector-Boson Production of Light Higgs Pairs in 2-Higgs Doublet Models,” arXiv:0706.4117 [hep-ph].
- [15] O. J. P. Eboli, G. C. Marques, S. F. Novaes and A. A. Natale, “TWIN HIGGS BOSON PRODUCTION,” *Phys. Lett. B* **197** (1987) 269.
- [16] A. Dobrovolskaya and V. Novikov, “On heavy Higgs boson production,” *Z. Phys. C* **52** (1991) 427.
- [17] A. Abbasabadi, W. W. Repko, D. A. Dicus and R. Vega, “SINGLE AND DOUBLE HIGGS PRODUCTION BY GAUGE BOSON FUSION,” *Phys. Lett. B* **213** (1988) 386.
- [18] A. Djouadi, W. Kilian, M. Muhlleitner and P. M. Zerwas, “Production of neutral Higgs-boson pairs at LHC,” *Eur. Phys. J. C* **10** (1999) 45 [arXiv:hep-ph/9904287].
- [19] S. L. Glashow and S. Weinberg, “Natural Conservation Laws For Neutral Currents,” *Phys. Rev. D* **15** (1977) 1958.
- [20] N. G. Deshpande and E. Ma, “Pattern Of Symmetry Breaking With Two Higgs Doublets,” *Phys. Rev. D* **18** (1978) 2574; S. Nie and M. Sher, “Vacuum stability bounds in the two-Higgs doublet model,” *Phys. Lett. B* **449** (1999) 89 [arXiv:hep-ph/9811234]; S. Kanemura, T. Kasai and Y. Okada, “Mass bounds of the lightest CP-even Higgs boson in the two-Higgs-doublet model,” *Phys. Lett. B* **471** (1999) 182 [arXiv:hep-ph/9903289].
- [21] B. W. Lee, C. Quigg and H. B. Thacker, “The Strength Of Weak Interactions At Very High-Energies And The Higgs Boson Mass,” *Phys. Rev. Lett.* **38** (1977) 883; B. W. Lee, C. Quigg and H. B. Thacker, “Weak Interactions At Very High-Energies: The Role Of The Higgs Boson Mass,” *Phys. Rev. D* **16** (1977) 1519; H. Huffel and G. Pocsik, “Unitarity Bounds On Higgs Boson Masses In The Weinberg-Salam Model With Two Higgs Doublets,” *Z. Phys. C* **8** (1981) 13; J. Maalampi, J. Sirkka and I. Vilja, “Tree Level Unitarity And Triviality Bounds For Two Higgs Models,” *Phys. Lett. B* **265** (1991) 371; A. G. Akeroyd, A. Arhrib and E. M. Naimi, “Note on tree-level unitarity in the general two Higgs doublet model,” *Phys. Lett. B* **490** (2000) 119 [arXiv:hep-ph/0006035].
- [22] E. Asakawa, O. Brein and S. Kanemura, “Enhancement of $W^+ H^-$ production at hadron colliders in the two Higgs doublet model,” *Phys. Rev. D* **72**, 055017 (2005) [arXiv:hep-ph/0506249].
- [23] S. Kanemura, T. Kubota and E. Takasugi, “Lee-Quigg-Thacker bounds for Higgs boson masses in a two doublet model,” *Phys. Lett. B* **313** (1993) 155 [arXiv:hep-ph/9303263].
- [24] D. Choudhury, T. M. P. Tait and C. E. M. Wagner, “Probing heavy Higgs boson models with a TeV linear collider,” *Phys. Rev. D* **65** (2002) 115007 [arXiv:hep-ph/0202162]; P. H. Chankowski, T. Farris, B. Grzadkowski, J. F. Gunion, J. Kalinowski and M. Krawczyk, “Do precision electroweak constraints guarantee $e^+ e^-$ collider discovery of at least one Higgs boson of a two Higgs doublet model?,” *Phys. Lett. B* **496**, 195 (2000) [arXiv:hep-ph/0009271].

- [25] W. M. Yao *et al.* [Particle Data Group], “Review of particle physics,” *J. Phys. G* **33** (2006) 1.
- [26] C. Georg, diploma thesis, <http://www-itp.particle.uni-karlsruhe.de/diplomatheses.de.shtml>;
J. R. Andersen and J. M. Smillie, “QCD and electroweak interference in Higgs production by gauge boson fusion,” *Phys. Rev. D* **75** (2007) 037301 [arXiv:hep-ph/0611281].
- [27] J. R. Andersen, T. Binoth, G. Heinrich and J. M. Smillie, “Loop induced interference effects in Higgs Boson plus two jet production at the LHC,” *JHEP* **0802**, 057 (2008) [arXiv:0709.3513 [hep-ph]].
- [28] A. Bredenstein, K. Hagiwara and B. Jager, “Mixed QCD-electroweak contributions to Higgs-plus-dijet production at the LHC,” *Phys. Rev. D* **77** (2008) 073004 [arXiv:0801.4231 [hep-ph]].
- [29] K. Hagiwara and D. Zeppenfeld, “Helicity Amplitudes for Heavy Lepton Production in e^+e^- Annihilation,” *Nucl. Phys. B* **274** (1986) 1; K. Hagiwara and D. Zeppenfeld, “Amplitudes for Multiparton Processes Involving a Current at e^+e^- , $e^\pm p$, and Hadron Colliders,” *Nucl. Phys. B* **313** (1989) 560.
- [30] T. Hahn, “A Mathematica interface for FormCalc-generated code,” arXiv:hep-ph/0611273; T. Hahn and J. I. Illana, “Excursions into FeynArts and FormCalc,” *Nucl. Phys. Proc. Suppl.* **160** (2006) 101 [arXiv:hep-ph/0607049]; T. Hahn and M. Rauch, “News from FormCalc and LoopTools,” *Nucl. Phys. Proc. Suppl.* **157** (2006) 236 [arXiv:hep-ph/0601248]; T. Hahn, “New developments in FormCalc 4.1,” *In the Proceedings of 2005 International Linear Collider Workshop (LCWS 2005), Stanford, California, 18-22 Mar 2005, pp 0604* [arXiv:hep-ph/0506201]; T. Hahn, “Optimizations for the computation of radiative corrections,” *Nucl. Phys. Proc. Suppl.* **116** (2003) 363 [arXiv:hep-ph/0210220]; T. Hahn and M. Perez-Victoria, “Automatized one-loop calculations in four and D dimensions,” *Comput. Phys. Commun.* **118** (1999) 153 [arXiv:hep-ph/9807565].
- [31] T. Hahn, “Generating Feynman diagrams and amplitudes with FeynArts 3,” *Comput. Phys. Commun.* **140** (2001) 418 [arXiv:hep-ph/0012260]; T. Hahn and C. Schappacher, “The implementation of the minimal supersymmetric standard model in FeynArts and FormCalc,” *Comput. Phys. Commun.* **143** (2002) 54 [arXiv:hep-ph/0105349]. J. Kublbeck, M. Bohm and A. Denner, “FEYN ARTS: COMPUTER ALGEBRAIC GENERATION OF FEYNMAN GRAPHS AND AMPLITUDES,” *Comput. Phys. Commun.* **60** (1990) 165.
- [32] S. Catani and M. H. Seymour, “A general algorithm for calculating jet cross sections in NLO QCD,” *Nucl. Phys. B* **485** (1997) 291 [Erratum-ibid. **B510**, 503 (1997)] [hep-ph/9605323].
- [33] W. Siegel, “Supersymmetric Dimensional Regularization Via Dimensional Reduction,” *Phys. Lett. B* **84** (1979) 193; W. Siegel, “Inconsistency Of Supersymmetric Dimensional Regularization,” *Phys. Lett. B* **94** (1980) 37.
- [34] S. Catani, Yu. L. Dokshitzer and B. R. Webber, “The K-perpendicular clustering algorithm for jets in deep inelastic scattering and hadron collisions,” *Phys. Lett. B* **285** (1992) 291; S. Catani, Yu. L. Dokshitzer, M. H. Seymour and B. R. Webber, “Longitudinally invariant K(t) clustering algorithms for hadron hadron collisions,” *Nucl. Phys. B* **406** (1993) 187; S. D. Ellis and D. E. Soper, “Successive combination jet algorithm for hadron collision,” *Phys. Rev. D* **48** (1993) 3160
- [35] G. C. Blazey *et al.*, “Run II jet physics,” hep-ex/0005012.

- [36] J. Pumplin, D. R. Stump, J. Huston, H. L. Lai, P. Nadolsky and W. K. Tung, “New generation of parton distributions with Uncertainties from Global QCD Analysis ,” *J. High Energy Phys.* **07** (2002) 012 [[hep-ph/0201195](#)].
- [37] V. Hankele, G. Klamke, D. Zeppenfeld and T. Figy, “Anomalous Higgs boson couplings in vector boson fusion at the CERN LHC,” *Phys. Rev. D* **74** (2006) 095001 [[arXiv:hep-ph/0609075](#)].
- [38] T. Figy and D. Zeppenfeld, “QCD corrections to jet correlations in weak boson fusion,” *Phys. Lett. B* **591** (2004) 297 [[arXiv:hep-ph/0403297](#)].
- [39] P. Konar and D. Zeppenfeld, “Next-to-leading order QCD corrections to slepton pair production via vector-boson fusion,” *Phys. Lett. B* **647** (2007) 460 [[arXiv:hep-ph/0612119](#)].